

SANDIA REPORT

Printed November, 2023



Sandia
National
Laboratories

Parameter estimation for incidence angle modifier models for photovoltaic modules

Abigail R. Jones, Clifford W. Hansen, Kevin S. Anderson

Prepared by
Sandia National Laboratories
Albuquerque, New Mexico 87185
Livermore, California 94550

Issued by Sandia National Laboratories, operated for the United States Department of Energy by National Technology & Engineering Solutions of Sandia, LLC.

NOTICE: This report was prepared as an account of work sponsored by an agency of the United States Government. Neither the United States Government, nor any agency thereof, nor any of their employees, nor any of their contractors, subcontractors, or their employees, make any warranty, express or implied, or assume any legal liability or responsibility for the accuracy, completeness, or usefulness of any information, apparatus, product, or process disclosed, or represent that its use would not infringe privately owned rights. Reference herein to any specific commercial product, process, or service by trade name, trademark, manufacturer, or otherwise, does not necessarily constitute or imply its endorsement, recommendation, or favoring by the United States Government, any agency thereof, or any of their contractors or subcontractors. The views and opinions expressed herein do not necessarily state or reflect those of the United States Government, any agency thereof, or any of their contractors.

Printed in the United States of America. This report has been reproduced directly from the best available copy.

Available to DOE and DOE contractors from

U.S. Department of Energy
Office of Scientific and Technical Information
P.O. Box 62
Oak Ridge, TN 37831

Telephone: (865) 576-8401
Facsimile: (865) 576-5728
E-Mail: reports@osti.gov
Online ordering: <http://www.osti.gov/scitech>

Available to the public from

U.S. Department of Commerce
National Technical Information Service
5301 Shawnee Road
Alexandria, VA 22312

Telephone: (800) 553-6847
Facsimile: (703) 605-6900
E-Mail: orders@ntis.gov
Online order: <https://classic.ntis.gov/help/order-methods>



ABSTRACT

We present methods to estimate parameters for models for the incidence angle modifier for simulating irradiance on a photovoltaic array. The incidence angle modifier quantifies the fraction of direct irradiance that is reflected away at the array's face, as a function of the direct irradiance's angle of incidence. Parameters can be estimated from data and the fitting method can be used to convert between models. We show that the model conversion procedure results in models that produce similar annual insolation on a fixed plane.

CONTENTS

1. Introduction	7
2. Model fitting	9
2.1. Residual function and weights	9
2.2. Minimization	10
3. Model conversion	11
3.1. Converting to the ASHRAE or Martin-Ruiz models	11
3.2. Converting to the physical model	11
3.2.1. Converting from Martin-Ruiz to physical	12
3.2.2. Converting from ASHRAE to physical	12
4. Algorithm Performance	15
4.1. Numerical convergence	15
4.2. Convergence to the global minimum	16
4.3. Model incompatibility	16
4.4. Validation of equivalent insolation	18
4.5. The default weight function	20
5. Approximate Transfer Functions	25
6. Conclusion	27
References	29
Appendix	31
Distribution	37

LIST OF FIGURES

Figure 4-1. Transfer functions for source and target model parameters.	17
Figure 4-2. Residuals for conversion of the Martin-Ruiz model to the physical model.	18
Figure 4-3. Illustration of compatible and incompatible model curves.	19
Figure 4-4. Incompatible physical and Martin-Ruiz models.	20
Figure 4-5. Influence of weight functions on the relative absolute difference in annual insolation for source and target models.	22
Figure 4-6. Jumps in fitted IAM model as source parameter evolves.	23
Figure A-1. Residuals for conversion of the Martin-Ruiz model to the ASHRAE model.	31
Figure A-2. Residuals for conversion of the ASHRAE model to the physical model.	32
Figure A-3. Residuals for conversion of the ASHRAE model to the Martin-Ruiz model.	33
Figure A-4. Residuals for conversion of the physical model to the ASHRAE model.	34
Figure A-5. Residuals for conversion of the physical model to the Martin-Ruiz model.	35

LIST OF TABLES

Table 2-1. Parameter bounds and guesses for each IAM model fitting.	10
Table 3-1. Parameter bounds and guesses for each IAM model conversion.	11
Table 4-1. Parameter ranges for each IAM model.	15
Table 4-2. Statistics for large residuals.	16
Table 4-3. Statistics for comparison of annual insolation.	20

1. INTRODUCTION

The incidence angle modifier (IAM) quantifies the fraction of direct sunlight that is transmitted through the surface of a PV module, normalized by the transmittance at normal incidence. As the angle between the sun and the surface of the panel increases, the reflected direct irradiance increases and the IAM decreases correspondingly.

Several models can be used to quantify the IAM. Each model requires one or more parameters that are determined from measurements. We focus here on three popular models: the ASHRAE model [1], the Martin-Ruiz model [2], and the physical model [3], all of which are implemented in pvlib-python [4].

We describe each of these three models below. In each equation, θ is the angle of incidence of the direct sunlight on the module.

The ASHRAE model is described by the following equation, where b is a parameter.

$$\text{IAM}(\theta; b) = 1 - b \left(\frac{1}{\cos(\theta)} - 1 \right) \quad (1)$$

The Martin-Ruiz IAM model is described by the following equation, where a_r is a parameter.

$$\text{IAM}(\theta; a_r) = \frac{1 - \exp(-\cos(\theta)/a_r)}{1 - \exp(-1/a_r)} \quad (2)$$

The physical model is derived by applying the Fresnel equations to a system with a single material interface. This model is described by the following equation, where n is the index of refraction of the cover glass, K is the glazing extinction coefficient (1/meters), L is the glazing thickness (meters), and $\theta_r = \arcsin\left(\frac{1}{n} \sin(\theta)\right)$.

$$\text{IAM}(\theta; n, K, L) = \frac{\exp\left(-\frac{K \cdot L}{\cos(\theta_r)}\right) \left[1 - \frac{1}{2} \left(\frac{\sin^2(\theta_r - \theta)}{\sin^2(\theta_r + \theta)} + \frac{\tan^2(\theta_r - \theta)}{\tan^2(\theta_r + \theta)} \right) \right]}{\exp(-K \cdot L) \left[1 - \left(\frac{1-n}{1+n} \right)^2 \right]} \quad (3)$$

2. MODEL FITTING

The ASHRAE and Martin-Ruiz models each require one empirical parameter, denoted as b and a_r , respectively. The physical model requires three parameters, n , K , and L , which have physical interpretation. However, we regard these parameters as empirical and determine values by fitting to data. This approach is justified because the physical model's equation is an ideal representation of reflections in a system with a single interface, whereas PV modules comprise several layers of materials with complex reflection behavior.

Fitting a candidate model to data entails minimizing a sum of residuals, i.e., differences between the model and data, with a weight possibly associated with each residual. The choice of residual function, weights, and optimization procedure all influence the derived parameters.

2.1. Residual function and weights

We want a residual function that measures “closeness” of a model to data on the domain $0^\circ \leq \theta \leq 90^\circ$. We want a residual function that performs well for each model. The residual function should also lend itself to minimization.

In addition, we want a residual function such that a converted model produces similar plane-of-array (POA) insolation as a source model in a simulation of a PV system. Because the IAM curve described by each model differs, we cannot rely on a close fit for every θ value. Simply minimizing a sum of residuals over the domain $0^\circ \leq \theta \leq 90^\circ$ may yield a target model that underfits the source model at lower values of aoi that are more significant for insolation, in order to force a closer fit at higher values of aoi . Thus, we introduce weighting to the residual function.

Let weights be a function that takes in a value for θ between 0° and 90° and outputs the weight associated with that angle. Then, fixing choices for the parameters of the source and target models, the residual function is

$$\sum_{\theta \in S} (|source(\theta) - target(\theta)| \cdot weights(\theta)), \quad (4)$$

where S is some sampling of θ values. We chose the absolute value of the difference between source and target models over squaring the difference because squaring the difference resulted in a residual surface that was quite flat near the minimum, making it sometimes difficult to find the minimum value.

The particular choice of weight function influences the optimized parameters. We opted to use $weights(\theta) = 1 - \sin(\theta)$ for reasons that will be discussed later. In our code we include an option to pass a weight function when converting between models to allow users to customize the conversion.

2.2. Minimization

We minimize the residual function (4) by using SciPy’s [5] multivariable optimization functionality in `optimize.minimize`. Although both the ASHRAE and Martin-Ruiz models have a single parameter, and so, when we are converting to either of these models, we could have chosen to use a function specifically designed for single variable optimization. However, to streamline the code, we chose to use `optimize.minimize` throughout.

`optimize.minimize` offers a number of methods. We chose Powell’s method for two reasons: Powell’s method does not require derivatives, and it allows for bounded optimization in SciPy version 1.5.0 and above. In our case, bounding the target parameters is important to avoid parameters that would give nonsense IAM values, such as $a_r < 0$ in the Martin-Ruiz model. Bounded optimization also lets us focus the optimizer on particular parameter regions, which helps with finding better (and more physically reasonable) values for the target model’s parameters.

The bounded version of `optimize.minimize(method='powell')` takes at least three arguments: the function we want to minimize with some number of unknowns, an initial guess of the minimum’s location, and bounds for each unknown.

Table 2-1 summarizes parameter bounds and initial guesses for fitting each model. In the case of the physical model, the parameters L and K always appear as a product. Hence we optimize only for L , and fix $K = 4$, which is the glazing extinction coefficient for “water white” glass [3]. For glass, typically $4 \leq K \leq 32$ [6] but it can be expected that glass used for PV modules will be as transmissive as possible. As a consequence of fixed $K = 4$, the bounds for L are wider than might otherwise be expected (recall that L is measured in meters, and the upper limit of 8 cm is much greater than typical for PV modules).

Table 2-1 Parameter bounds and guesses for each IAM model fitting.

Model	Parameter Bounds	Initial Guess
ASHRAE	$1 \times 10^{-8} \leq b \leq 1$	$b = 0.05$
Martin-Ruiz	$1 \times 10^{-8} \leq a_r \leq 1$	$a_r = 0.05$
physical	$1 \leq n \leq 2$ $0 \leq L \leq 0.08$	$n = 1 + 1 \times 10^{-8}$ $L = 0.002$

3. MODEL CONVERSION

Here, we present an algorithm to convert between models. We convert from a source model with given parameters to a target model by calculating IAM values from the source model and selecting parameters for the target model by minimizing the weighted residual function (4) over the range $0^\circ \leq \theta \leq 90^\circ$. We implement the algorithm in Python. For each pair of source and target model, bounds and initial guesses are summarized in Table 3-1.

Table 3-1 Parameter bounds and guesses for each IAM model conversion.

Source	Target	Parameter Bounds	Initial Guess
ASHRAE	Martin-Ruiz physical	$1 \times 10^{-4} \leq a_r \leq 1$ $1 \times 10^{-6} \leq L \leq 0.08$ $0.8 \leq n \leq 2$ (when n is not calculated from ASHRAE intercept)	$a_r = 1 \times 10^{-3}$ $L = 0.002$ $n = 1.0$
Martin-Ruiz	ASHRAE physical	$1 \times 10^{-4} \leq b \leq 1$ $1 \times 10^{-6} \leq L \leq 0.08$ $1.05 \leq n \leq 2$	$b = 1 \times 10^{-3}$ $L = 0.002$ $n = 1.1$
physical	ASHRAE Martin-Ruiz	$1 \times 10^{-4} \leq b \leq 1$ $1 \times 10^{-4} \leq a_r \leq 1$	$b = 1 \times 10^{-3}$ $a_r = 1 \times 10^{-3}$

3.1. Converting to the ASHRAE or Martin-Ruiz models

When converting to a model that has only one parameter, i.e., the ASHRAE or Martin-Ruiz model, the parameter bounds and initial guess do not play a significant role in the minimization; the residual curve often has a very clear minimum which `optimize.minimize` does not struggle to find. For this reason, we choose relatively wide parameter bounds: a lower bound of 10^{-4} and an upper bound of 1.0. Both b for the ASHRAE model and a_r for the Martin-Ruiz model tend to values between 0.1 and 0.2. We set the initial guess for either b or a_r to 10^{-3} . Conversions to the ASHRAE and Martin-Ruiz models required no other massaging to produce decent results.

3.2. Converting to the physical model

Converting to the physical model requires finding multiple parameters: n , K , and L . In this case, some preparatory work improves the conversions dramatically. We optimize only for L , and fix $K = 4$. Other aspects of the conversion depend on the source model.

3.2.1. **Converting from Martin-Ruiz to physical**

Converting from the Martin-Ruiz model to the physical model relies on understanding a bit about Powell's method. A simplified description of Powell's method follows.

1. Take an initial guess and bounds.
2. Associate a direction vector with each unknown. (In our case, we used the standard basis vectors for \mathbb{R}^2 as direction vectors.)
3. For each unknown:
 - a) Fixing the other unknowns at their current guess values, minimize the residual by varying the current unknown along its direction vector (making sure to stay within the unknown's bounds).
 - b) Store the optimized parameter.
4. Update direction vectors as necessary.
5. Repeat until terminating conditions are met.

Because the parameters for the target model are updated sequentially in each iteration, the order in which we optimize each unknown *can* matter, even if our choice of direction vectors suggests that the values can be chosen independently. We found that, when the Martin-Ruiz model parameter a_r is less than 0.22 good results were obtained when L was optimized first, but when $a_r > 0.22$ good results required n to be optimized first. Doing the optimization with the variables in the other order resulted in `optimize.minimize` getting stuck in a region of parameters for the physical model that fit poorly to the source model.

We start the optimization with the initial guess $n = 1$ and $L = 0.002$. We bound $1.05 \leq n \leq 2$ and $10^{-6} \leq L \leq 0.08$.

3.2.2. **Converting from ASHRAE to physical**

The ASHRAE model often has an x -intercept less than 90° , whereas when $n > 1$, the x -intercept for the physical model is at 90° . Because of this, we allow physically unreasonable values, i.e., $n < 1$, to force the physical model's intercept to coincide with the ASHRAE model's intercept. This choice often considerably improves agreement with the ASHRAE model. Since non-physical values of n may not be of interest to all users, we have provided an option in the code to not choose n in this manner.

In order to force the physical model to have an x -intercept less than 90° , we fix $n = \sin(\theta_0)$, where θ_0 is the desired x -intercept. The x -intercept of the physical model is determined by the second factor in the numerator. The x -intercept is located where this is zero, requiring θ and n so that

$$2 = \frac{\sin^2(\theta_r - \theta)}{\sin^2(\theta_r + \theta)} + \frac{\tan^2(\theta_r - \theta)}{\tan^2(\theta_r + \theta)}. \quad (5)$$

(Recall that $\theta_r = \arcsin(\frac{1}{n} \sin(\theta))$.) When $n > 1$ both the sine term and the tangent term are bounded by one on $0^\circ \leq \theta \leq 90^\circ$. Thus, their sum equals two only when both terms equal one. This occurs exactly when $\theta = 90^\circ$ ¹. Thus, for $n > 1$, the physical model's x -intercept will always be at $\theta = 90^\circ$.

For a fixed $\theta_0 < 90^\circ$, we can choose $n < 1$ so that the physical model's x -intercept is at θ_0 . We do this by making θ_r as close to 90° as possible². Setting $\theta_r = 90^\circ$ and solving for n in terms of θ_0 then yields $n = \sin(\theta_0)$, as desired.

When n is set by the ASHRAE model's intercept, we set bounds $10^{-6} \leq L \leq 0.08$ and set the initial guess to $L = 0.002$. When n is not set by the ASHRAE model's intercept, we set bounds for n to be $0.8 \leq n \leq 2$. For the ASHRAE model, the order of iteration in Powell's method is L first, then n .

¹Showing this requires the trigonometric identity $\sin(x + 180^\circ) = -\sin(x)$, and recalling that tangent has a period of 180° .

²Showing that this choice makes the above sum equal two requires the trigonometric identities $\sin(90^\circ \pm x) = \cos(x)$ and $\tan(90^\circ \pm x) = \mp \cot(x)$.

4. ALGORITHM PERFORMANCE

We examine the performance of the conversion algorithm in three ways. First we examine how well `optimize.minimize` converges with its default settings. Second, we simulate a PV system and compare the POA insolation after removing reflected direct irradiance predicted by the source and target models. Finally, we use the comparison of POA insolation to justify our choice of a weight function.

4.1. Numerical convergence

We examine numerical convergence of the target model's parameters by reducing the tolerance of `optimize.minimize` and comparing between the optimized parameters.

For each of the six possible source-target model pairs, we discretize the ranges shown in Table 4-1 with 300 equally spaced points to obtain a sample of source model parameters. For each element of the sample, we convert to the target model using the default tolerance³ of 1×10^{-3} and again with 1×10^{-12} and compute the relative difference in the resulting target model parameters. This test of convergence demonstrates the success (or failure) of the algorithm at finding a minimum set of parameters using the default tolerance.

Table 4-1 Parameter ranges for each IAM model.

	Lower Bound	Upper Bound
ASHRAE		
b	0.02	0.2
Martin-Ruiz		
a_r	0.08	0.25
physical		
n	1	1.7
K	4	4
L	10^{-6}	0.01

Table 4-2 summarizes the results of the convergence analysis, listing the percentage of each sample where the maximum absolute relative difference in any parameter exceeds 10^{-4} , and the average of the large relative differences.

Except for converting between the Martin-Ruiz and the physical model, the default settings obtain parameters within 0.01% of the highly-converged values for most of the source model's parameter range. Even when converting between the Martin-Ruiz and the physical model, the returned parameters are within a few percent of the highly converged values. We conclude that the default settings provide adequate convergence.

³xtol, relative absolute tolerance for each parameter at the minimum point.

Source Model	Target Model	Rel. Diff. $> 10^{-4}$	Avg. of Large Parameter Difference
ASHRAE	Martin-Ruiz	13%	1.41×10^{-4}
	physical	0%	N/A
Martin-Ruiz	ASHRAE	14%	1.94×10^{-3}
	physical	40%	4.05×10^{-2}
physical	ASHRAE	1.3%	1.52×10^{-2}
	Martin-Ruiz	33%	2.27×10^{-4}

Table 4-2 Statistics for large residuals.

Figure 4-1 shows the relationship between source and target model parameters. In each case, the target model parameters are smooth functions of the source model parameters, promoting confidence in the robustness of the conversion algorithm.

4.2. Convergence to the global minimum

We examine convergence to the global minimum of the residual function by plotting the residual for the source-target model pair over a wide range of the target model's parameter space. This examination gives us confidence that the resulting target model fits the source model as well as can be expected. This confidence is needed in cases where the source and target models differ considerably, as then we can conclude that no significant improvements to the optimization algorithm can be made; the curves described by the two models are just incompatible.

We map the residual function for converting the source model to the target model by selecting values for the source model parameters, discretizing the target model's parameter space (using 300 points for each parameter) and computing the residual for each point. We also convert the source to the target model and plot the residual for the converted model.

Figure 4-2 illustrates the convergence for the Martin-Ruiz to physical model conversion; plots for other source-target pairs are found in the Appendix. In most cases, the converted model's residual agrees closely with the minimum residual found in the parameter space grid. At high values of a_r , the two residuals diverge somewhat. However, high values of a_r are of little practical interest.

4.3. Model incompatibility

Sometimes, the fitted target model does not appear to fit the source model very well. However, by verifying that the algorithm is finding the global minimum of the residual function, we know that this choice of parameters is indeed optimal. In these situations, the models are simply incompatible.

Figure 4-3 illustrates compatible and incompatible models. The top row displays a successful conversion from the physical to the Martin-Ruiz model, and the bottom row shows a conversion where

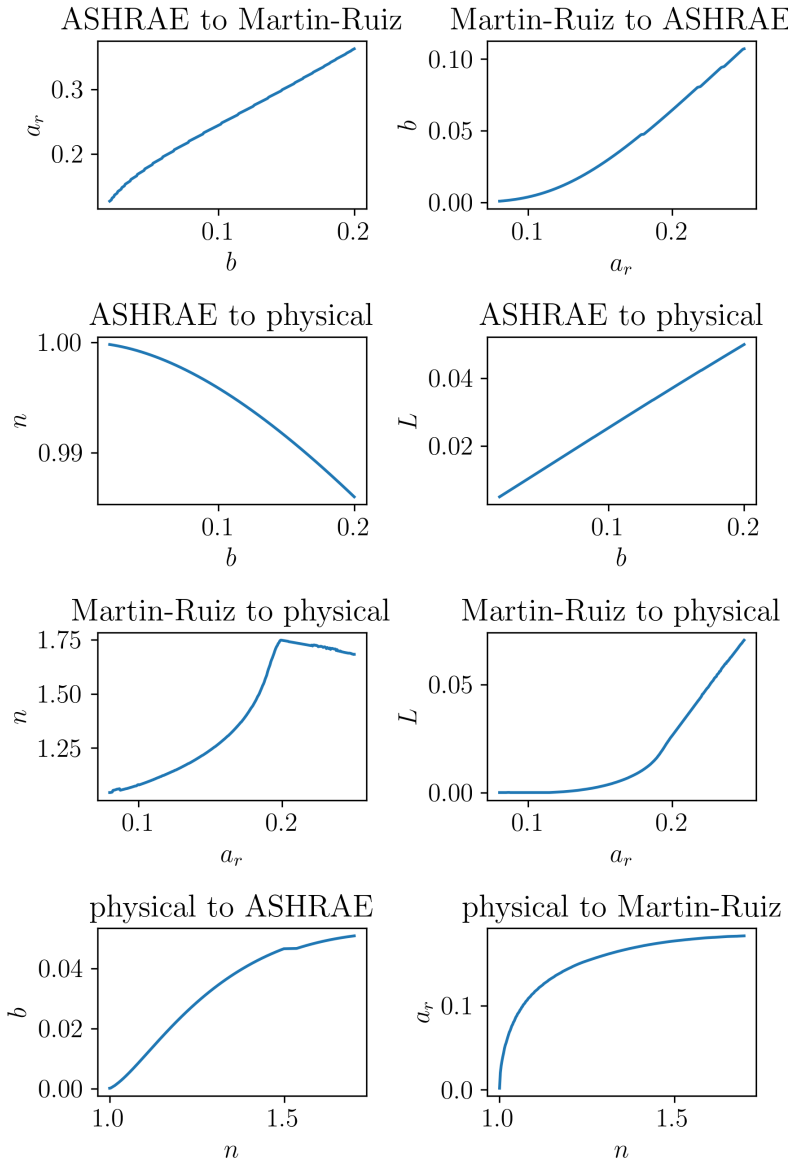


Figure 4-1 Transfer functions for source and target model parameters.

the best-fitting Martin-Ruiz model deviates from the source physical model. In both conversions the algorithm has successfully found the global minimum of the residual.

The reason for model incompatibility can be visualized by varying the Martin-Ruiz model parameter away from its best-fitting value. Figure 4-4 illustrates AOI vs. IAM curves for the best-fitting model ($a_r = 0.1278$) and for a_r at 70% and 150% of the best-fitting value. None of the three Martin-Ruiz models is able to closely match the source physical model. This incompatibility can occur when converting between any pair of models, but generally at the extremes of the source model's range of parameters. In this illustration, the source physical model's index of refraction n is very low (1.0059).

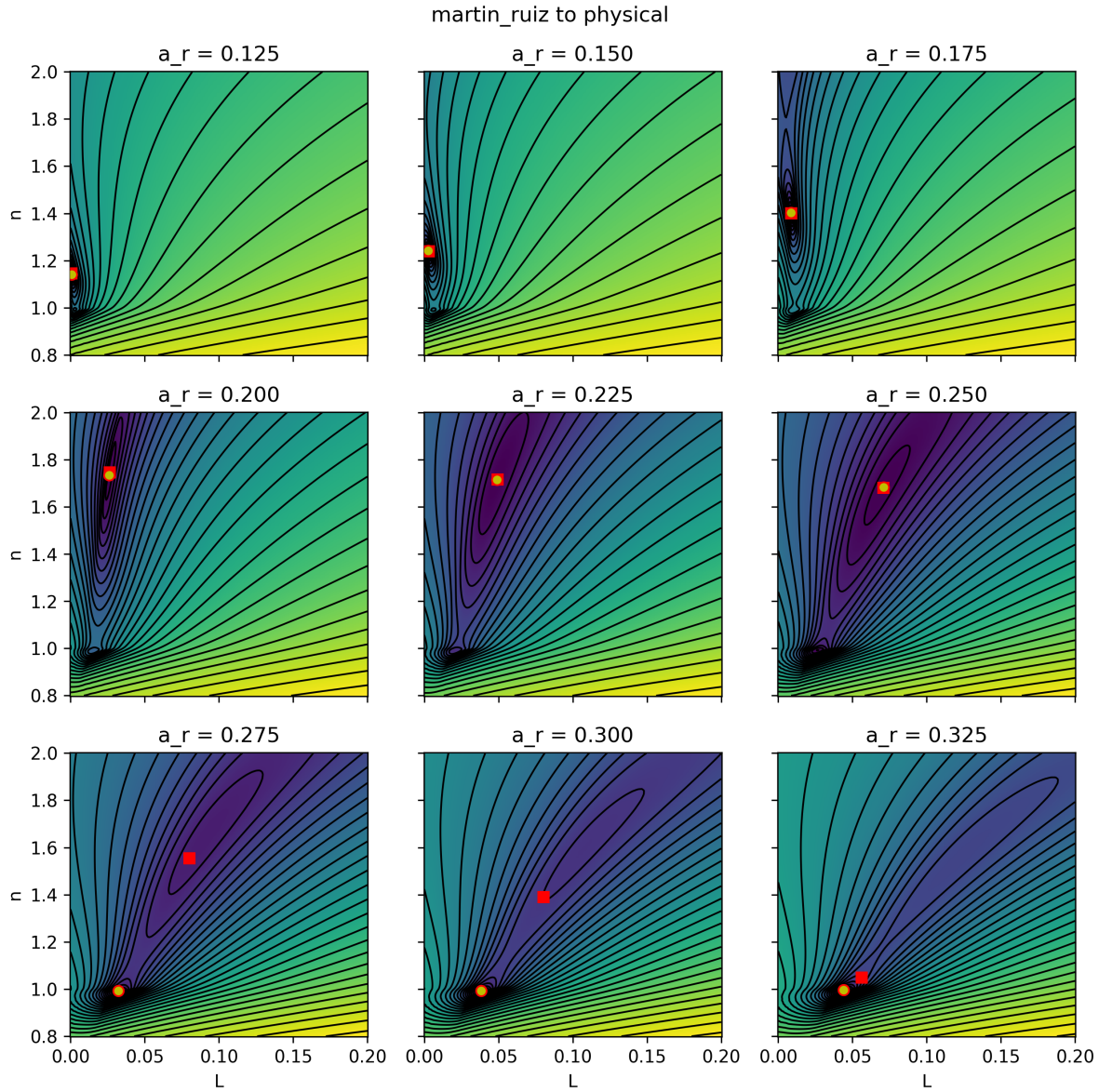


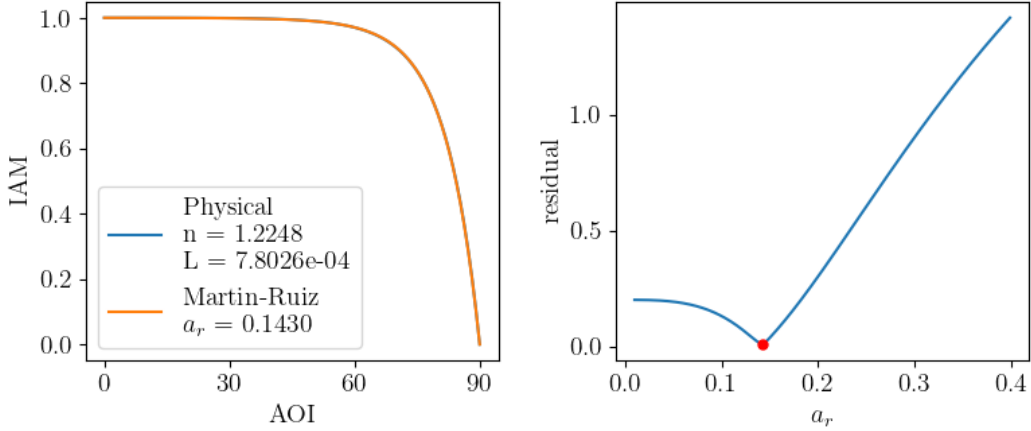
Figure 4-2 Residuals for conversion of the Martin-Ruiz model to the physical model.

Red square indicates the converted model. Yellow circle indicates the minimum residual in the grid.

4.4. Validation of equivalent insolation

To validate the equivalence of the source and target models, we compare POA insolation after applying both models to reduce direct irradiance for reflections. We first define two reference PV systems located in Albuquerque, NM, oriented south at either latitude tilt or horizontal. We then randomly sample parameters for a source model (using the same intervals as in table 4-1) and find parameters for the target model. For each reference system we compute the POA insolation for a full year, assuming clear-sky conditions to compute irradiance using the Ineichen clear-sky model

A compatible conversion



An incompatible conversion

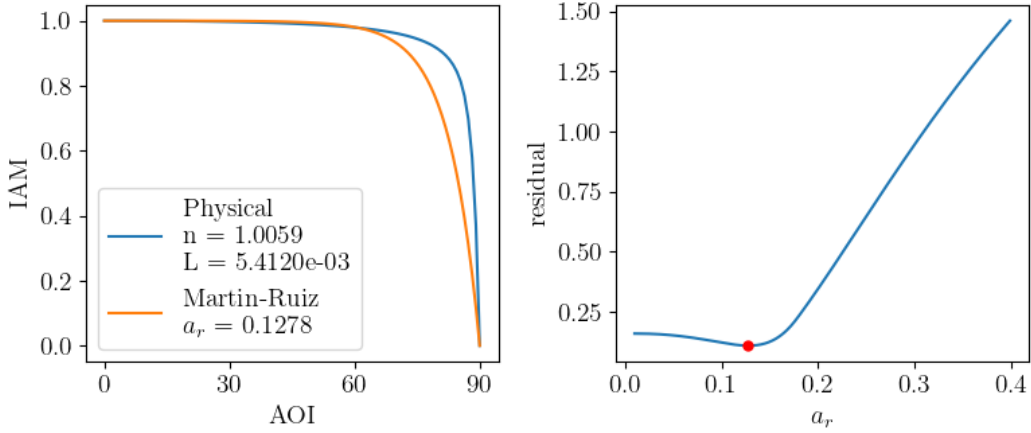


Figure 4-3 Illustration of compatible and incompatible model curves.

[7] and transposing irradiance to the array's plane using the Hay-Davies transposition model [8]. We apply the IAM from each model to the direct irradiance in the plane-of-array and then compute each model's POA insolation, after reflection loss. Finally, we compute the relative difference in POA insolation as

$$\frac{|\text{target insolation} - \text{source insolation}|}{\text{source insolation}}$$

We consider two models as equivalent if the relative difference is less than 0.001, as this difference would indicate a relative difference of less than 0.1% in the annual electrical energy modeled for the reference systems.

For each of the six possible pairs of source and target model, we repeat this process 100 times. Table 4-3 summarizes the results, giving the average and median relative difference, the percentage of

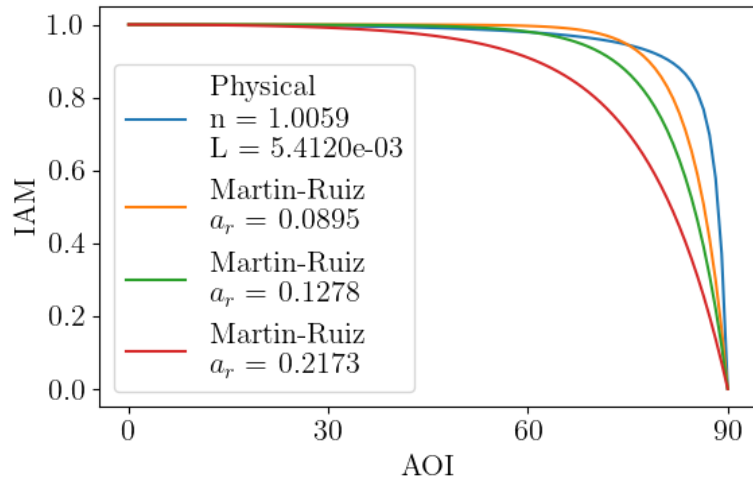


Figure 4-4 Incompatible physical and Martin-Ruiz models.

the simulations in which the relative difference exceeds 0.001 (exceptions), and the average relative difference for the exceptions.

Table 4-3 Statistics for comparison of annual insolation.

source	target	average	median	% of exceptions	avg. of exceptions
ASHRAE	Martin-Ruiz	0.000480	0.000321	16.7%	0.00126
	physical	0.000140	0.000164	0%	N/A
Martin-Ruiz	ASHRAE	0.000568	0.000663	0%	N/A
	physical	0.000419	8.67×10^{-5}	19%	0.00144
physical	ASHRAE	0.000299	0.000249	1.6%	0.00136
	Martin-Ruiz	0.000401	0.000291	8.0%	0.00137

The averages and medians of the relative differences are often much smaller than 0.001. Even for the exceptions (samples with relative insolation difference exceeding 0.001) the average relative difference is less than 0.0015. Thus, for almost every possible conversion, we can be confident that the source model and target model output equivalent POA insolation.

4.5. The default weight function

The validations described above use the default weight function, $\text{weight}(\theta) = 1 - \sin(\theta)$. We consider here different choices of weight function and examine how the weight function affects the

relative absolute difference in POA insolation between the source model and target models⁴. We found that $1 - \sin(\theta)$ minimizes the relative differences more often than other weight functions we considered.

Other weight functions we consider are

$$\begin{aligned} \text{no weight}(\theta) &= 1 \\ \text{cosine}(\theta) &= \cos(\theta) \\ \text{step}(\theta) &= \begin{cases} 1 & \text{if } \theta \leq 60 \\ 0 & \text{if } \theta > 60. \end{cases} \end{aligned}$$

For each of the six possible pairs of source and target model, we vary the source model's parameters over the intervals given in Table 4-1 and compute the relative differences in insolation as explained in Section 4.4⁵. We repeat this process for each of the four possible weight functions. Figure 4-5 summarizes the results and indicates combinations of weight functions and source parameter values where the relative difference exceeds 0.001.

When considering all six plots, the curves associated with $1 - \sin(\theta)$ most consistently remain below the horizontal line at 0.001. However, it should be noted that the step function also performed quite well, and sometimes even outperformed $1 - \sin(\theta)$. This suggests that there are a number of weight functions that could reasonably be chosen in order to preserve insolation output. We choose $1 - \sin(\theta)$ as the default weight function. Other weight functions could be chosen that preserve different properties of the models.

Some curves involving the ASHRAE model (e.g., the "no weight" curve in the ASHRAE to physical plot) show a sawtooth appearance where relative insolation changes systematically over some parameter interval, then changes dramatically at some threshold parameter value. The sawtooth pattern does not result from the relatively coarse sample of 100 (the sawtooth persists in plots with a sample of size 1000). The pattern is due to shifts in the best-fitting target model, which may not occur smoothly as the source parameters evolve, and which are more pronounced when greater weights are assigned to residuals at high AOI values. Figure 4-6 illustrates how the best-fitting physical model jumps as the ASHRAE model parameter b evolves across one of these thresholds for the "no weight" weight function. The difference between the ASHRAE and fitted physical model is very similar for $b = 0.178$ and $b = 0.180$ but jumps to a new profile when $b = 0.182$. Such non-smooth shifts in the fitted physical model translate to shifts in the reflected direct irradiance, and thence to shifts in the insolation ratio. When the weight function de-emphasizes residuals at large AOI, the shifts are less pronounced (as with $1 - \sin(\theta)$) or are smoothed away (with the "step" weight function).

⁴Difference is relative to insolation when using the source model

⁵When the source model is the physical model, we only vary n and fixed $K = 4$ and $L = 0.002$.

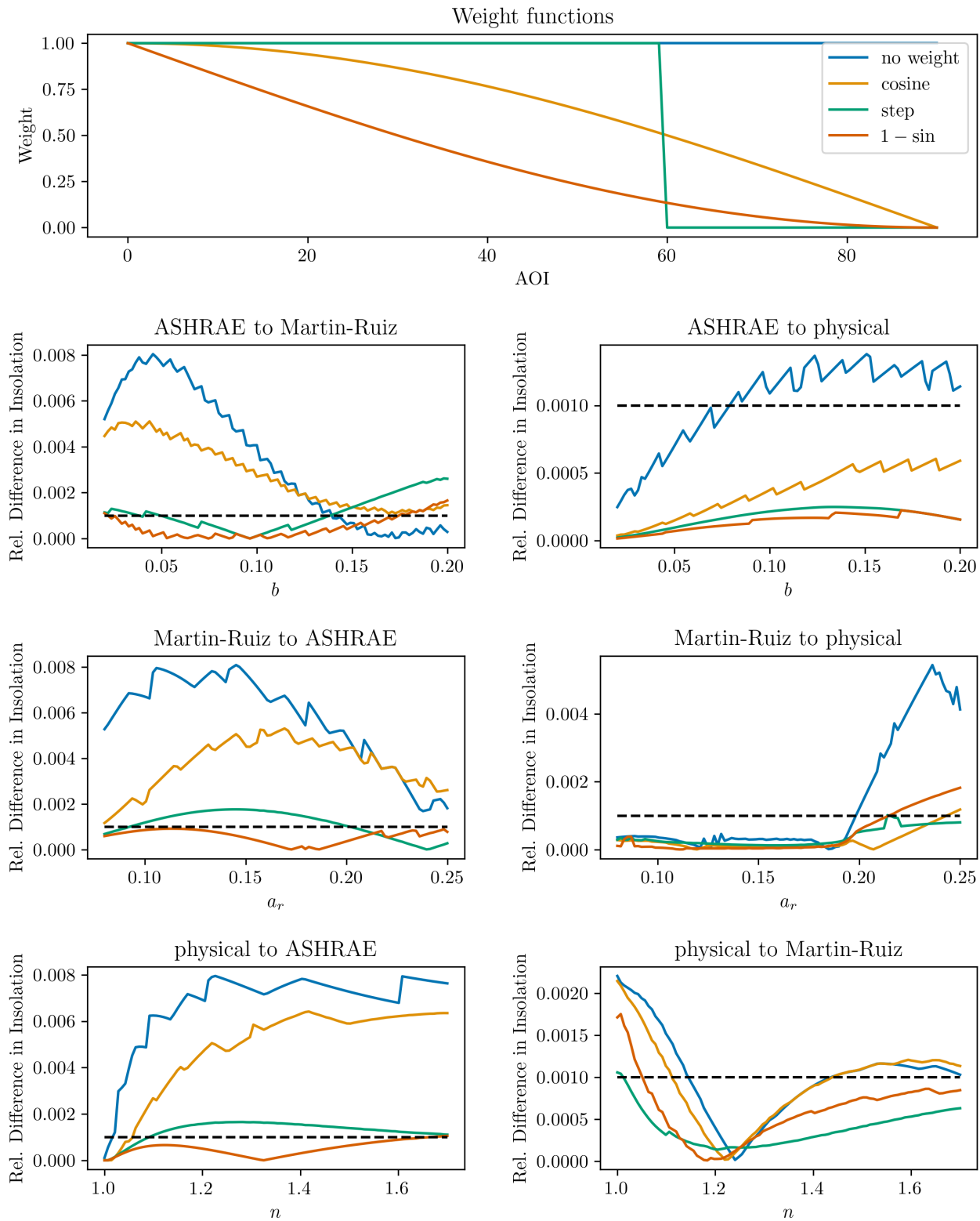


Figure 4-5 Influence of weight functions on the relative absolute difference in annual insolation for source and target models.

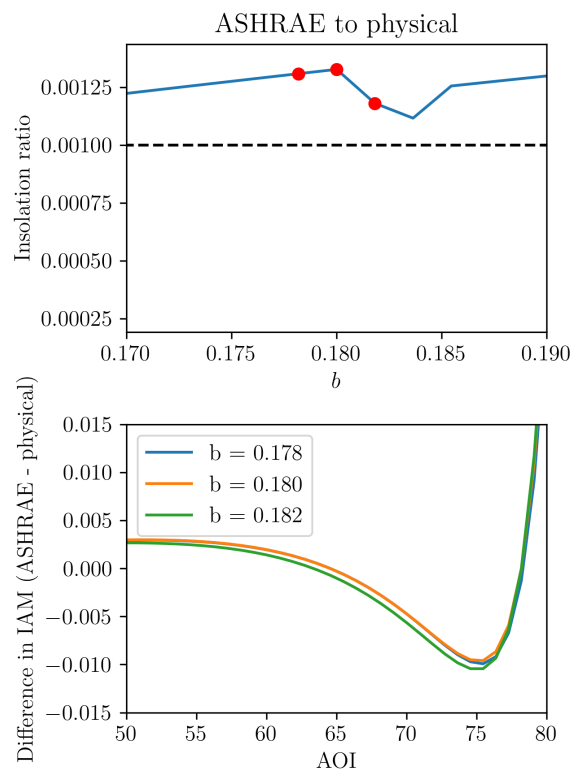


Figure 4-6 Jumps in fitted IAM model as source parameter evolves.

5. APPROXIMATE TRANSFER FUNCTIONS

Here we provide approximate transfer functions based on the transfer curves produced by the numerical optimization method (Figure 4-1). These approximate functions are intended to be a more convenient alternative to running the numerical optimization method. Note that these functions were fit to values determined using the default residual function and weighting scheme.

First, converting a_r to the other models:

$$n(a_r) \approx \begin{cases} 2.904 - 65.99a_r + 843.2a_r^2 - 4615.0a_r^3 + 9553.0a_r^4 & 0.08 \leq a_r < 0.198 \\ 2.008 - 1.299a_r & 0.198 \leq a_r < 0.25 \end{cases} \quad (6)$$

$$L(a_r) \approx \begin{cases} 1 \cdot 10^{-6} & 0.08 \leq a_r < 0.1175 \\ 0.3239 - 9.13a_r + 96.28a_r^2 - 453.4a_r^3 + 814.4a_r^4 & 0.1175 \leq a_r < 0.19 \\ -0.1544 + 0.9032a_r & 0.19 \leq a_r < 0.25 \end{cases} \quad (7)$$

$$b(a_r) \approx \begin{cases} 0.004534 + 0.08397a_r - 5.394a_r^2 + 57.12a_r^3 - 123.9a_r^4 & 0.08 \leq a_r < 0.195 \\ -0.1078 + 0.8647a_r - 0.01867a_r^2 & 0.195 \leq a_r < 0.25 \end{cases} \quad (8)$$

Over the specified a_r range, these equations approximate n to within ± 0.015 , L to within ± 0.0006 , and b to within ± 0.0001 .

Now, converting n and L (with K fixed at 4, as usual) to a_r and b :

$$a_r(n, L) \approx \frac{4.915 \cdot 10^{-5} + 0.6180L}{n - 0.9702} - 4.1071 + 10.679n - 10.134n^2 + 4.319n^3 - 0.69491n^4 \quad (9)$$

$$b(n, L) \approx \frac{-0.231 - 47.7L}{n(L - 70.19) + 59.6} - 0.5265 + 0.8787n - 0.4568n^2 + 0.0799n^3 \quad (10)$$

Over the ranges n from 1.1 to 1.8 and L from 10^{-6} to 10^{-2} , these equations predict a_r to within ± 0.002 and b to within ± 0.001 .

Finally, converting b to the other models:

$$a_r(b) \approx \begin{cases} 0.008002 + 10.33b - 304.5b^2 + 4753.0b^3 - 27980b^4 & 0.01 \leq b < 0.06 \\ 0.128 + 1.153b + 0.09767b^2 & 0.06 \leq b < 0.20 \end{cases} \quad (11)$$

$$n(b) \approx 1.0 - 0.002616b - 0.4447b^2 + 0.5381b^3 \quad (12)$$

$$L(b) \approx 0.0001434 + 0.2506b \quad (13)$$

Over the range 0.01 to 0.2, these equations approximate n to within ± 0.00005 , L to within ± 0.0003 , and a_r to within ± 0.0015 .

6. CONCLUSION

The presented algorithms allow for fitting of three common models for describing the incidence angle modifier (IAM) for a PV system, and for conversion between these models. For the fitting methods we recommend, we provide transfer functions to compute a target model's parameters directly from the source model's parameters. The converted model's IAM does not always closely follow the IAM of the source model. However, we demonstrate that the converted model produces annual insolation in the plane-of-array (after reflections) that is comparable to that produced from the source model, indicating that the two models would also produce equivalent energy when simulating a PV system.

REFERENCES

- [1] A.F. Souka and H.H. Safwat. Determination of the optimum orientations for the double-exposure, flat-plate collector and its reflectors. *Solar Energy*, 10(4):170–174, 1966.
- [2] N. Martin and J.M. Ruiz. Calculation of the pv modules angular losses under field conditions by means of an analytical model. *Solar Energy Materials and Solar Cells*, 70(1):25–38, 2001.
- [3] W. De Soto, S.A. Klein, and W.A. Beckman. Improvement and validation of a model for photovoltaic array performance. *Solar Energy*, 80(1):78–88, 2006.
- [4] William F. Holmgren, Clifford W. Hansen, and Mark A. Mikofski. pvlib python: a python package for modeling solar energy systems. *Journal of Open Source Software*, 3(29):884, 2018.
- [5] Pauli Virtanen, Ralf Gommers, Travis E. Oliphant, Matt Haberland, Tyler Reddy, David Cournapeau, Evgeni Burovski, Pearu Peterson, Warren Weckesser, Jonathan Bright, Stéfan J. van der Walt, Matthew Brett, Joshua Wilson, K. Jarrod Millman, Nikolay Mayorov, Andrew R. J. Nelson, Eric Jones, Robert Kern, Eric Larson, C J Carey, İlhan Polat, Yu Feng, Eric W. Moore, Jake VanderPlas, Denis Laxalde, Josef Perktold, Robert Cimrman, Ian Henriksen, E. A. Quintero, Charles R. Harris, Anne M. Archibald, Antônio H. Ribeiro, Fabian Pedregosa, Paul van Mulbregt, and SciPy 1.0 Contributors. SciPy 1.0: Fundamental Algorithms for Scientific Computing in Python. *Nature Methods*, 17:261–272, 2020.
- [6] Robert E. Parkin. A note on the extinction coefficient and absorptivity of glass. *Solar Energy*, 114:196–197, 2015.
- [7] Pierre Ineichen and Richard Perez. A new airmass independent formulation for the linke turbidity coefficient. *Solar Energy*, 73(3):151–157, 2002.
- [8] P.G. Loutzenhiser, H. Manz, C. Felsmann, P.A. Strachan, T. Frank, and G.M. Maxwell. Empirical validation of models to compute solar irradiance on inclined surfaces for building energy simulation. *Solar Energy*, 81(2):254–267, 2007.

APPENDIX

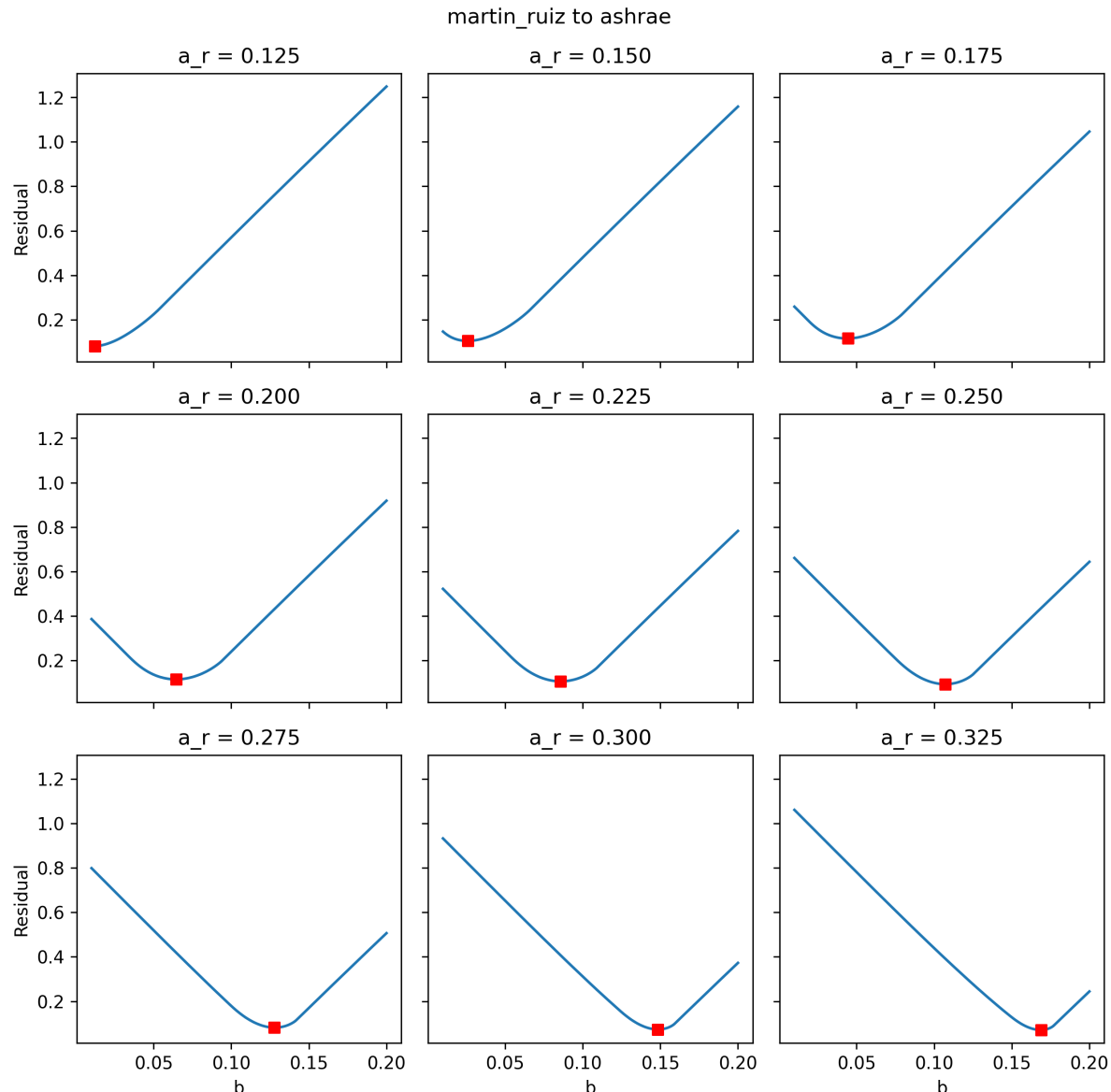


Figure A-1 Residuals for conversion of the Martin-Ruiz model to the ASHRAE model.

Red square indicates the converted model.

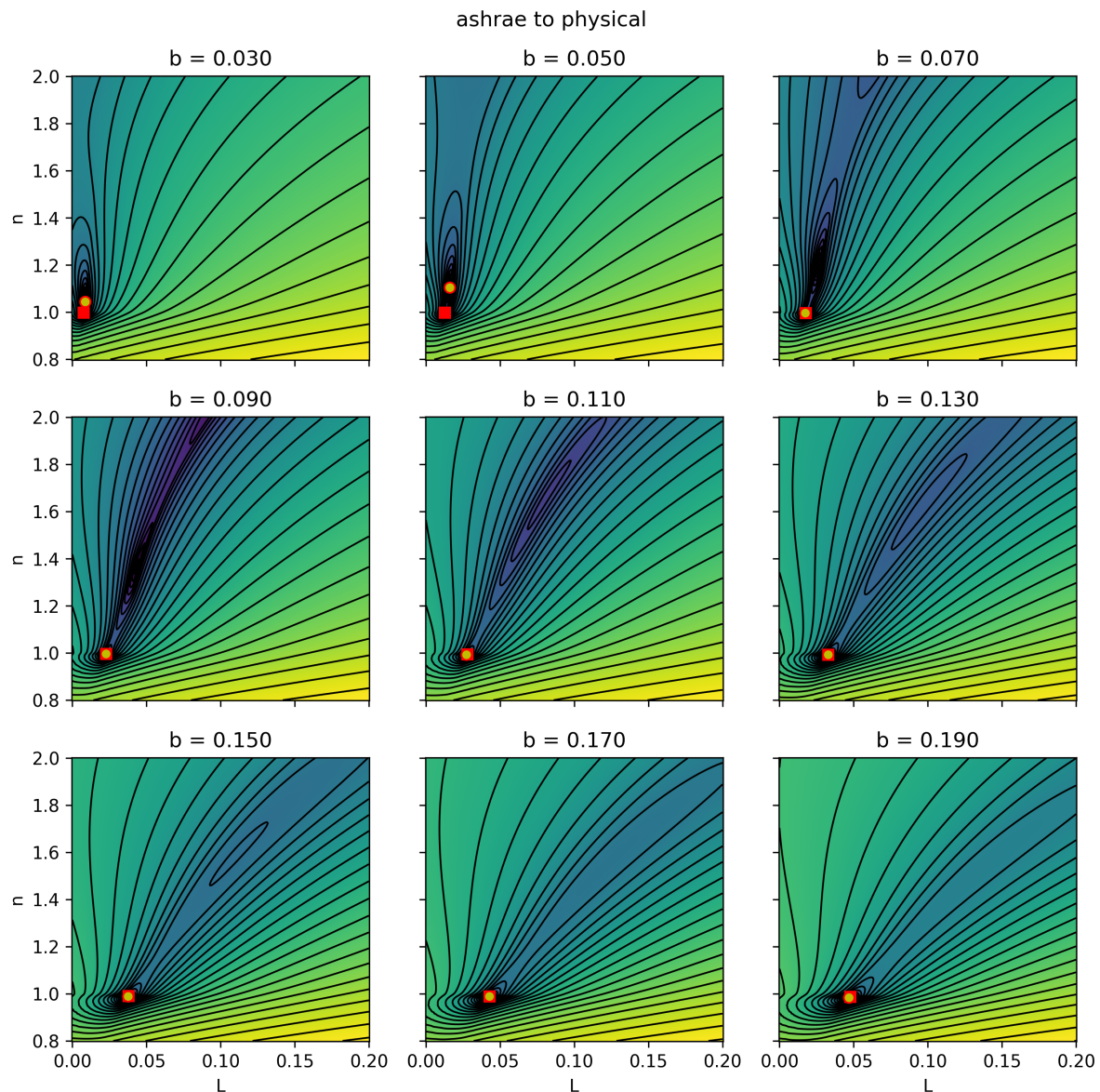


Figure A-2 Residuals for conversion of the ASHRAE model to the physical model.

Red square indicates the converted model. Yellow circle indicates the minimum residual in the grid.

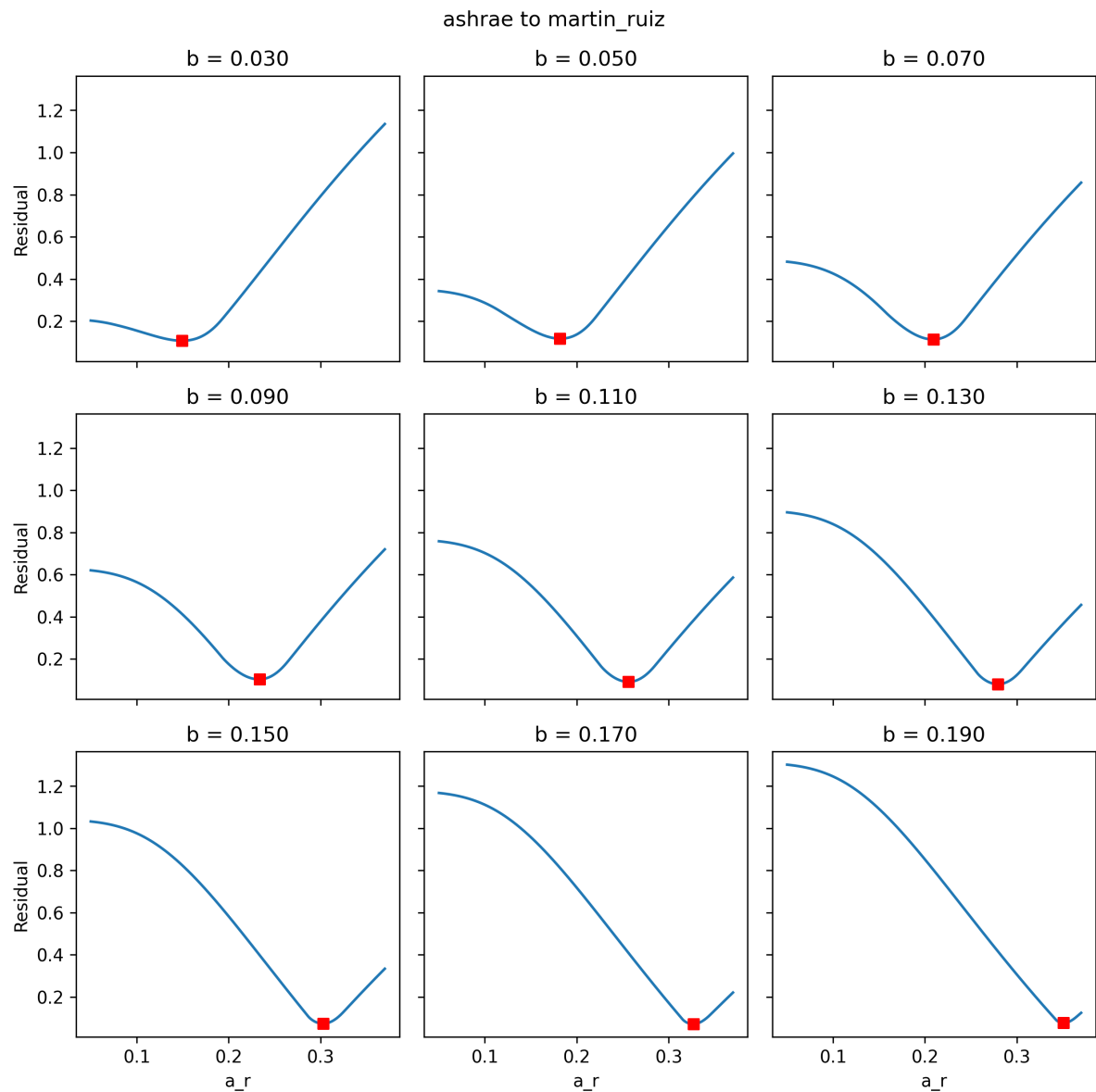


Figure A-3 Residuals for conversion of the ASHRAE model to the Martin-Ruiz model.

Red square indicates the converted model.

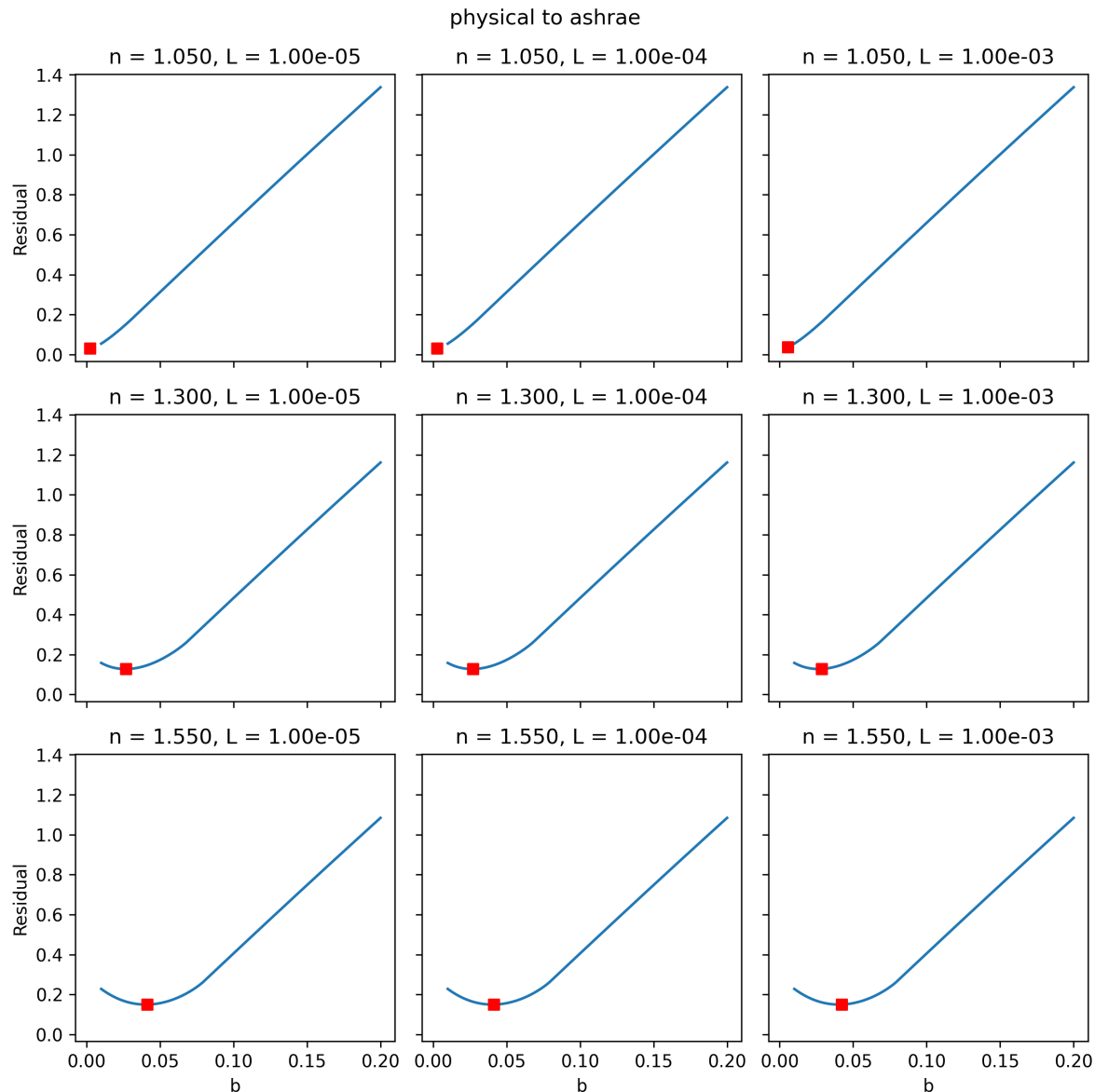


Figure A-4 Residuals for conversion of the physical model to the ASHRAE model.

Red square indicates the converted model.

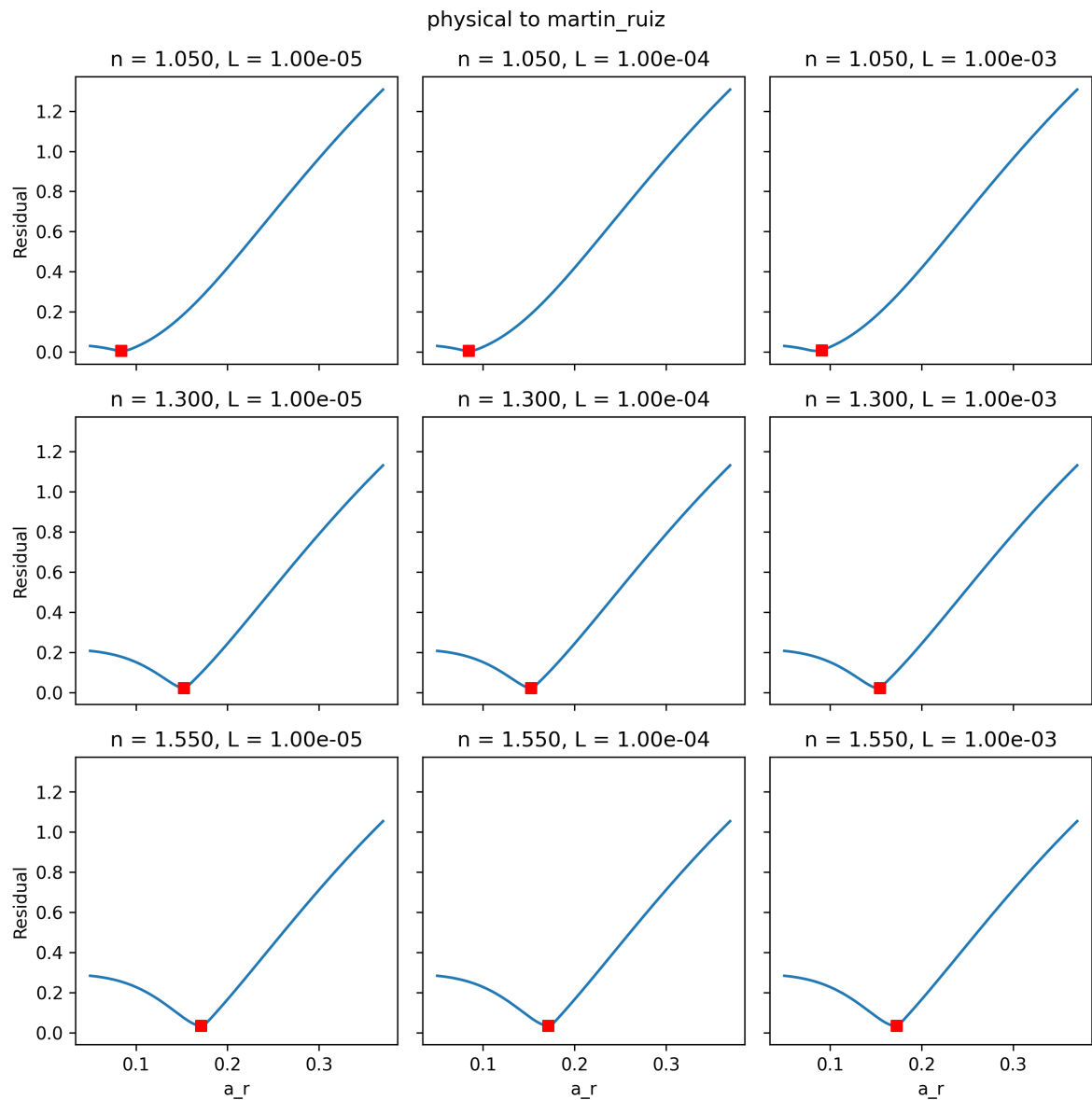


Figure A-5 Residuals for conversion of the physical model to the Martin-Ruiz model.

Red square indicates the converted model.

DISTRIBUTION

Email—Internal

Name	Org.	Sandia Email Address
Technical Library	1911	sanddocs@sandia.gov



**Sandia
National
Laboratories**

Sandia National Laboratories is a multimission laboratory managed and operated by National Technology & Engineering Solutions of Sandia LLC, a wholly owned subsidiary of Honeywell International Inc., for the U.S. Department of Energy's National Nuclear Security Administration under contract DE-NA0003525.